

Cite this: *Green Chem.*, 2011, **13**, 3453www.rsc.org/greenchem

PAPER

Stabilization of Cu(0)-nanoparticles into the nanopores of modified montmorillonite: An implication on the catalytic approach for “Click” reaction between azides and terminal alkynes†

Bibek Jyoti Borah,^a Dipanka Dutta,^a Partha Pratim Saikia,^b Nabin Chandra Barua^b and Dipak Kumar Dutta^{*a}

Received 18th August 2011, Accepted 13th September 2011

DOI: 10.1039/c1gc16021d

In situ generation of Cu(0)-nanoparticles in the nanopores of modified montmorillonite and their catalytic activity in 1,3-dipolar cycloaddition reactions between azides and terminal alkynes to synthesise 1,2,3-triazoles have been carried out. The modification of montmorillonite was carried out by activation with H₂SO₄ under controlled conditions for generating nanopores to act as a “host” for the Cu(0)-nanoparticles, which is executed by successful loading of Cu(CH₃COO)₂ metal precursor through an incipient wetness impregnation technique followed by reduction with NaBH₄. A TEM study reveals that Cu(0)-nanoparticles within the size range of 0–10 nm are evenly distributed on the support. The synthesized Cu(0)-nanoparticles exhibit face centered cubic (fcc) lattice geometry and serve as an efficient green catalyst for the “Click” azide–alkyne cycloaddition to afford highly regioselective 1,4-disubstituted 1,2,3-triazoles with excellent yields and selectivity in aqueous medium. The nanocatalysts can be recycled and reused several times without significant loss of their catalytic activity.

1. Introduction

Nanomaterials have aroused much interest in recent times because of their intriguing properties different from those of their corresponding bulk materials.¹ The development of metal and metal oxide nanoparticles is intensively pursued because of their importance for both fundamental science and advanced technology.^{1,2} The possibility of exploring the potential of nanoparticle-based materials as catalyst precursors for green organic synthesis is a challenge for researchers.³ In the present work, we have reported the application of modified montmorillonite clay supported Cu(0)-nanoparticles as an efficient alternative catalyst for the Cu(I)-catalysed “Click” azide–alkyne cycloaddition, which gives highly regioselective 1,4-disubstituted 1,2,3-triazoles. 1,2,3-triazoles are basically five membered nitrogen heterocyclic compounds, stable to moisture, oxygen, light and also metabolism in the body, which show biological activities, including anti-HIV, antiallergic, antifungal

and antimicrobial.⁴ They have also found wide industrial applications as photostabilizers, agrochemicals, optical brighteners, corrosion inhibitors *etc.*⁴ Therefore, tremendous attention has been given to develop new protocols for the synthesis of 1,2,3-triazoles after the pivotal discovery by the groups of Meldal and Sharpless,^{4a,5} in which Cu(I) efficiently catalyzed the reaction under mild conditions to give 1,4-disubstituted 1,2,3-triazoles. As the reaction meets the set of stringent criteria required in “Click” chemistry, Sharpless *et al.*^{4a} named it as the “Click” reaction. In spite of these, triazoles can be prepared by the cycloaddition of azides with electron deficient alkynes, metal acetylides, phosphonium salts and various substituted alkynes.⁶ Triazoles are also synthesized by using solid supports, like polymer, zeolite or resin bound azides, alkynes, enamines or β -ketoamides.⁷

Recently, considerable effort has also been devoted to the application of Cu(0)/Cu-oxide-nanoparticles as substitutes of bulk Cu metal in the title reaction in order to reduce the catalyst loading, reaction time and also to minimize the undesired products.⁸ The size and shape of nanoparticles as well as the nature of supporting materials on which the nanoparticles are stabilized are of the utmost importance for providing a highly active surface for catalysis. Sarkar *et al.*^{8a} have reported the use of PVP-stabilized Cu(0)-nanoparticles as a reusable catalyst for the “Click” reaction between terminal alkynes and azides in nonaqueous solvents. Kantam *et al.*^{8b} have synthesized 1,2,3-triazoles using alumina supported Cu(0)-nanoparticles as

^aMaterials Science Division, Council of Scientific and Industrial Research-North East Institute of Science and Technology, Jorhat, 785 006, Assam, India. E-mail: dipakkrdutta@yahoo.com; Fax: +91-376-2370 011; Tel: +91-376-2370 081

^bNatural Products Chemistry Division, Council of Scientific and Industrial Research-North East Institute of Science and Technology, Jorhat, 785 006, Assam, India

† Electronic supplementary information (ESI) available. See DOI: 10.1039/c1gc16021d

the catalyst precursor. Alonso *et al.*^{8c,d} have also reported an efficient catalytic system for 1,3-dipolar cycloaddition of azides to terminal alkynes and widely illustrated the substrate tolerance of the catalyst, the disadvantage of this catalytic system is that, due to its homogeneous nature, the catalyst could not be reused. Molteni *et al.* also used mixed Cu/Cu-oxide nanoparticles as a catalyst for the “Click” azide–alkyne cycloaddition.^{8e}

Moreover, due to stringent and growing environmental regulations, the chemical industry needs the development of ecofriendly and sustainable synthetic methods. In the synthesis of metal nanoparticles by reduction of the corresponding metal ion salt solutions, there are three areas of opportunity to engage in green chemistry: (i) choice of solvent (ii) the reducing agent used and (iii) the nature of stabilizing agent.⁹ In this context, there has also been increasing interest in employing environmentally benign, cheap, easily available and robust support/stabilizer materials for the synthesis of metal nanoparticles. Herein, we report a procedure for synthesizing Cu(0)-nanoparticles using environmentally benign montmorillonite clay as a support, which is collected from the natural deposition in the western part of India. The virgin montmorillonite clay was purified and activated with mineral acid under controlled conditions to generate a matrix having high surface area and contain micro- and mesopores with diameter in the range 0–10 nm on the surface. These nano range pores act as the “host” for the *in situ* generation of Cu(0)-nanoparticles and also limit the growth of the particles up to the desired range.^{2c,10} The use of a heterogeneous catalyst in organic synthesis also complies with the requirement of green chemistry as it offers easy separation, recovery of the catalyst from the reaction products and its recyclability. The synthesized Cu(0)-nanoparticles act as heterogeneous catalysts for the “Click” 1,3- dipolar cycloaddition of terminal alkynes and azides at room temperature with water as a solvent. These nanoparticles maintain their catalytic efficiency for several cycles and serve as potential reusable catalyst.

2. Experimental

2.1. Materials and methods

Bentonite (procured from Gujarat, India) containing quartz, iron oxide *etc.* as impurities was purified by sedimentation¹¹ to collect the <2 μm montmorillonite rich fraction. The basal spacing (d_{001}) of the air dried samples was about 12.5 \AA . The specific surface area determined by N_2 adsorption was $101 \text{ m}^2 \text{ g}^{-1}$. The analytical oxides composition of the bentonite determined was SiO_2 : 49.42%; Al_2O_3 : 20.02%; Fe_2O_3 : 7.49%; MgO : 2.82%; CaO : 0.69%; Loss on ignition: 17.51%; others (Na_2O , K_2O and TiO_2): 2.05%.

The montmorillonite (Parent Mont.) was converted to the homoionic Na^+ -exchanged form by stirring in 2 M NaCl solution for about 78 h, washed and dialysed against distilled water until the conductivity of the water approached that of distilled water. The cation exchange capacity (CEC) was 1.26 meq per g of clay (sample dried at 120°C).

$\text{Cu}(\text{CH}_3\text{COO})_2$, NaBH_4 , sodium azide, 1-azidodecane, 1-azidoadamantane, terminal alkynes, aliphatic bromo compounds were purchased from Sigma-Aldrich, USA. All the reagents were used as supplied.

IR spectra ($4000\text{--}400 \text{ cm}^{-1}$) were recorded on KBr discs in a Perkin–Elmer system 2000 FT-IR spectrophotometer. ^{29}Si and ^{27}Al MAS NMR spectra were recorded in DSX 300 NMR spectrometer. Powder XRD spectra were recorded on a Rigaku, Ultima IV X-ray diffractometer from $2\text{--}80^\circ 2\theta$ using $\text{Cu-K}\alpha$ source ($\lambda = 1.54 \text{ \AA}$). Specific surface area, pore volume, average pore diameter were measured with the Autosorb-1 (Quantachrome, USA). Specific surface area of the samples were measured by adsorption of nitrogen gas at 77 K and applying the Brunauer–Emmett–Teller (BET) calculation. Prior to adsorption, the samples were degassed at 250°C for 3 h. Pore size distributions were derived from desorption isotherms using the Barrett–Joyner–Halenda (BJH) method. Scanning electron microscopy (SEM) images and energy dispersive X-ray spectroscopy (EDX) patterns were obtained with Leo 1430 vp operated at 3 and 10 kV. Prior to examination, the samples were coated with gold. Transmission electron microscopy (TEM) and high resolution transmission electron microscopy (HRTEM) images were recorded on a JEOL JEM-2011 electron microscope and the specimens were prepared by dispersing powdered samples in isopropyl alcohol, placing them on a carbon coated copper grid and allowing them to dry. The Cu contents were determined by Inductively Coupled Plasma Atomic Emission Spectroscopy (ICP-AES) using Perkin Elmer, OPTIMA 2000 instrument.

2.2. Preparation of Support

Purified Na-montmorillonite (10 g) was taken into a 250 ml three necked round bottom flask and 200 ml 4 M sulphuric acid was added to it. The resulting dispersion was refluxed for 1 h. After cooling, the supernatant liquid was discarded and the activated montmorillonite was repeatedly washed with deionised water and finally dried in an air oven at $50 \pm 5^\circ\text{C}$ over night to obtain the solid product. This activated montmorillonite was designated as AT-Mont.

2.3. Preparation of Cu(0)-nanoparticles

0.5 g of AT-Mont. was taken into a 100 ml beaker and 15 ml (0.254 mmol) aqueous solution of $\text{Cu}(\text{CH}_3\text{COO})_2$ was added slowly under vigorous stirring conditions. The stirring was continued for another 6 h followed by evaporation to dryness in a rotary evaporator. 0.3 g of dry clay– $\text{Cu}(\text{CH}_3\text{COO})_2$ composite was dispersed in 50 ml water in a 100 ml two necked round bottom flask and 10 ml aqueous solution of NaBH_4 (134 mg, 3.54 mmol) was then added slowly over 15 min in a nitrogen environment under constant stirring conditions. The reaction started immediately and the colour changed from blue to black, due to conversion of $\text{Cu}(\text{II})$ into $\text{Cu}(\text{0})$ -nanoparticles. The black solid mass was recovered and washed with distilled water for several times and then dried in a desiccator for 12 h. The sample thus prepared was designated as $\text{Cu}(\text{0})$ -Mont.

2.4. Preparation of 1-azidodecane and 1,6-diazidohexane

A stoichiometric quantity of NaN_3 (300 mg for 1-azidodecane or 533 mg for 1,6-diazidohexane) was dissolved in dry dimethyl formamide (50 ml) and the solution was stirred vigorously for about 10 min followed by addition of stoichiometric quantity *i.e.* 1000 mg (1 : 1) of respective bromoalkanes (*e.g.* 1-bromodecane

Table 1 Surface properties of different montmorillonite clay based support/catalysts

Samples	Surface properties of support/catalysts		
	Specific surface area (m ² g ⁻¹)	Average pore diameter (nm)	Specific pore volume (cm ³ g ⁻¹)
AT-Mont.	422	4.28	0.5849
<div style="display: flex; align-items: center; justify-content: center;"> <div style="text-align: center;"> ↓ Catalyst ↓ After run Fresh → </div> </div>	299	5.18	0.3874
Cu(0)-Mont.	1	253	0.3123
	2	235	0.2875
	3	227	0.2173

or 1,6-dibromohexane) to this mixture. After completion of the reaction (monitored by TLC, R_f 0.48, hexane), water (30 ml) was added to the reaction mixture. The mixture was then extracted with diethyl ether (30 ml) and washed with water. The aqueous phase was then extracted with ethyl acetate (30 ml). Both the organic phases were mixed together and dried over anhydrous Na₂SO₄ and concentrated. The products were purified by performing column chromatography using silica gel (60–120 mesh) with hexane as eluent.

2.5. Typical experimental procedure for the synthesis of 1,2,3-triazoles

Azide (1 mmol), alkyne (1 mmol), triethylamine (1 mmol) and 25 mg (0.05 mol %) Cu(0)-catalyst (Cu(0)-Mont.) were added to 10 ml water and the reaction mixture was stirred at room temperature for the stipulated time period (Table 3). After completion of the reactions (monitored by TLC, for R_f values and solvent systems, see supporting information†), ethyl acetate (10 ml) was added to the whole reaction mixture and the solid catalyst was separated from the mixture by filtering through a sinter funnel (G-3). The recovered catalyst was washed with acetone (30 ml), dried in a desiccator and stored for another consecutive reaction run. The organic extract was washed with water (30 ml), dried over Na₂SO₄ and concentrated to give the corresponding triazole product. The products were purified by simple crystallization (Et₂O) or by performing column chromatography using silica gel (60–120 mesh) with ethyl acetate and hexane as eluents. The products were characterized by standard analytical techniques such as (¹H & ¹³C) NMR, FTIR, elemental analysis, mass spectroscopy, melting point determination and all gave satisfactory results (see supporting information†).

3. Results and discussion

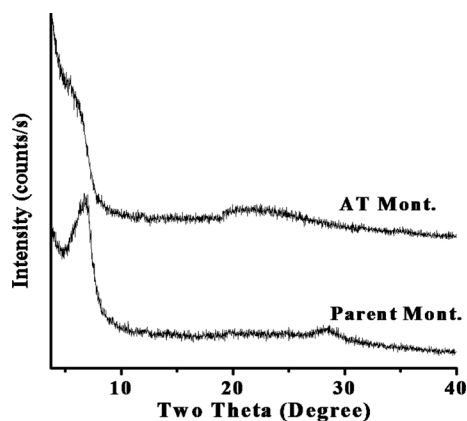
3.1. Characterization of Support

3.1.1. X-ray diffraction. The parent montmorillonite exhibited an intense basal reflection at 7.06° 2θ corresponding to a basal spacing of 12.5 Å (Fig. 1). The intensity of basal reflection decreases considerably after 1 h acid activation, which implies that the layered structure of the clay is disrupted and also a low intense broad reflection in the range 20–30° 2θ confirmed the formation of amorphous silica.¹²

3.1.2. Specific surface area and pore size distribution. The AT-Mont. contained micro- (<2 nm) and mesopores (2–50 nm)

Table 2 Cu(0)-nanoparticles catalyzed 1,3-dipolar cycloaddition of 1-azidodecane and phenylacetylene

Entry	Solvent	Et ₃ N used	Time (h)	Yield (%)
1a	Water : DCM (1 : 1)	Yes	1	80
1b	Water	No	1	0
		Yes	1	95
1c	Methanol	Yes	1	75
1d	Ethanol	Yes	1	70
1e	THF	Yes	1	65

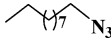
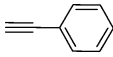
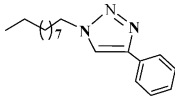
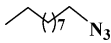
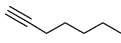
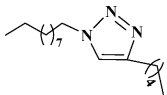
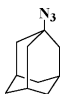
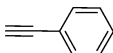
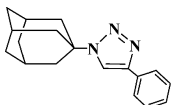
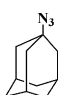
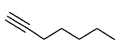
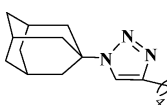
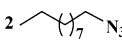
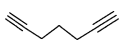
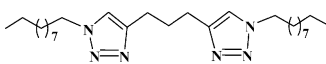
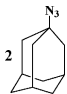
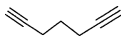
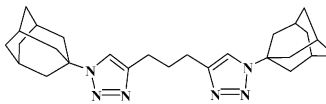
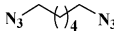
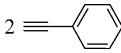
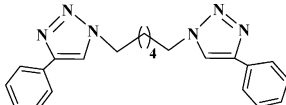
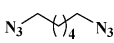
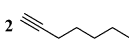
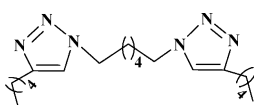
**Fig. 1** The powder XRD pattern of different montmorillonite.

with average pore diameters ~ 4.28 nm, a high specific surface area upto 422 m² g⁻¹ and a large specific pore volume of ~ 0.6 cm³ g⁻¹ (Table 1). The adsorption–desorption isotherm (Fig. 2) was of type-IV with a H3 hysteresis loop at P/P_0 ~ 0.4–0.9, indicating a mesoporous solid. The increase of surface area as well as pore volume is due to the leaching of Al from the clay matrix during acid activation, which also introduced permanent porosity on the clay surface. The differential volumes *versus* pore diameter plot (Fig. 2 (inset)) indicated relatively narrow pore size distributions and these nano range pores can be advantageously utilized for the *in situ* synthesis of various metal nanoparticles.^{2c,10}

3.1.3. FTIR spectra. The parent montmorillonite exhibited an intense absorption band at ~1034 cm⁻¹ for Si–O stretching vibrations of a tetrahedral sheet. The bands at 522 and 460 cm⁻¹

Table 3 1,3-dipolar cycloaddition of azides and alkynes catalyzed by Cu(0)-nanoparticles

$$\text{R}-\text{N}_3 + \text{C}\equiv\text{C}-\text{R}^1 \xrightarrow[\text{H}_2\text{O, Et}_3\text{N, Room Temp.}]{\text{Cu(0)-nanoparticles}} \text{R}-\text{N}(\text{N}=\text{N})-\text{C}(\text{R}^1)=\text{N}$$

Entry	Azide	Alkyne	Triazole	Time (h)	Yield (%)
1				1	95 ^a 90 ^b 86 ^c
2				1	89
3				1	92
4				1	87
5				1.5	92
6				1.5	90 ^a 85 ^b 83 ^c
7				1.5	85
8				1.5	88

^a 1st run, ^b 2nd run, ^c 3rd run

were due to Si–O–Al and Si–O–Si bending vibrations (see supporting information†). Acid activation shifted the band from ~1031 cm⁻¹ to ~1045 cm⁻¹. The appearance of a band near 795 cm⁻¹ indicated amorphous silica.¹³ Montmorillonite also showed absorption bands at 3634 cm⁻¹ due to stretching vibrations of the OH groups of Al–OH. The bands at 916, 875 and 792 cm⁻¹ were related to AlAl–OH, AlFe–OH and AlMg–OH vibrations.¹³ The disappearance of these bands during acid activation indicated the removal of Al, Fe and Mg ions from the clay mineral structure.

3.1.4. ²⁹Si and ²⁷Al MAS-NMR measurements. The parent montmorillonite showed an intense Si peak at about –93 ppm (Q³(OAl)), attributed to tetrahedral (3Si,Al) units of the octahedral sheet (see supporting information†). On acid activation for 1 h, the intensity of the peak at –93 ppm decreases and a new peak appeared at –111 ppm due to Q⁴ Si.

The ²⁷Al MAS-NMR spectra of parent montmorillonite exhibited an intense peak at 3.48 ppm and a weak peak at 67.39 ppm for octahedral and tetrahedral Al respectively (see supporting information†). During 1 h acid activation, the intensity of the octahedral Al peak decreased and shifted to 2.03 ppm while the tetrahedral Al peak remained unchanged.

3.1.5 SEM-EDX investigation. The typical SEM image of AT-Mont. (Fig. 3(A)) showed the formation of pores on the clay surface. The spot chemical analysis at the surface (Fig. 3(B)) revealed that predominant amounts of Si compare to Al were present on the surface. At the pores (Fig. 3(C)), only silica was present.

3.2. Characterization of Cu(0)-nanoparticles

The evidence of formation of Cu(0)-nanoparticles was obtained from powder XRD analysis. The Fig. 4 shows three broad peaks

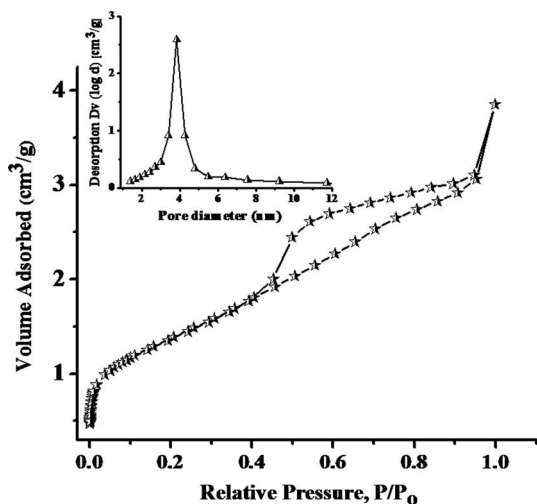


Fig. 2 N_2 adsorption/desorption isotherm and BJH pore size distribution curve (inset) of AT-Mont.

of 2θ values 43.3 , 50.3 and 74.1° which are assigned to the (111), (200) and (220) indices of face centered cubic (fcc) lattice of metallic Cu.^{8a,b,d} The XRD peaks for any other oxidation states of Cu were not observed, only those that could be attributed to the presence of Cu in the zero oxidation state.

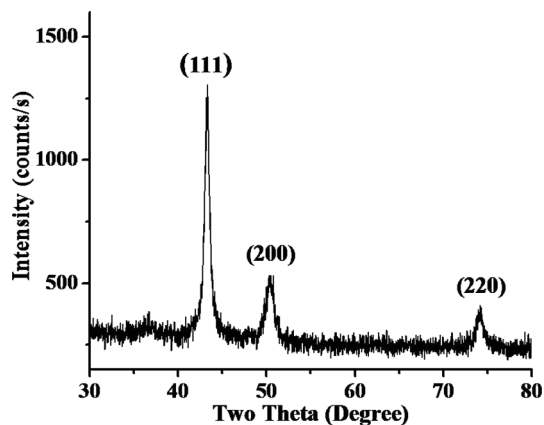
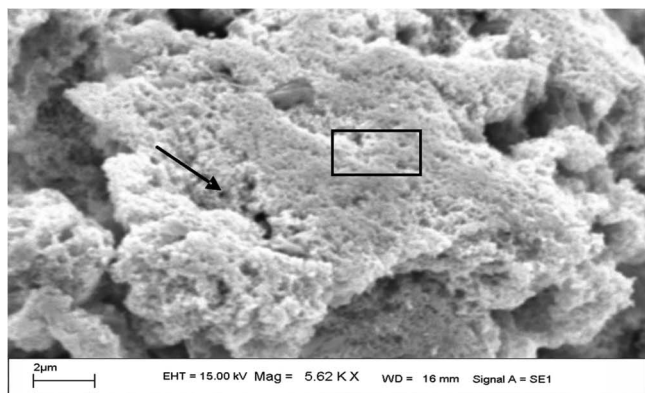
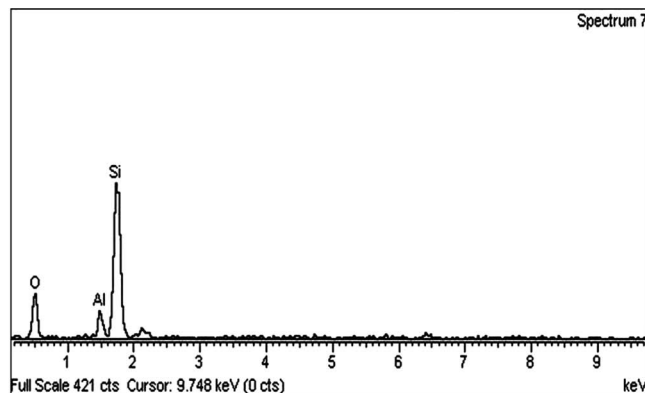


Fig. 4 The powder XRD pattern of Cu(0)-Mont.

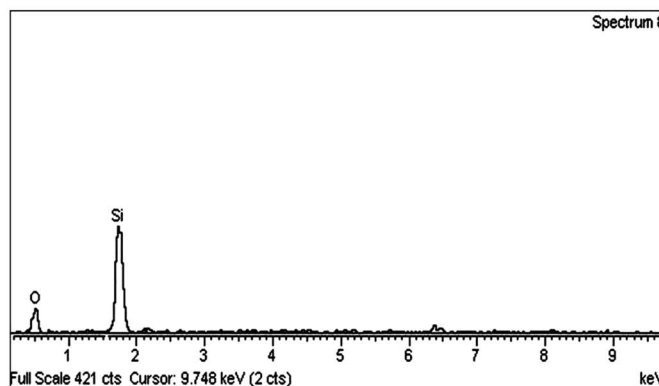
The TEM image (Fig. 5) of nanoparticles composites showed that dispersed Cu(0)-nanoparticles were formed in the micro- and mesopores of AT-Mont. The supported Cu(0)-nanoparticles were spherical in shape, well separated from each other and with sizes of below 10 nm. From the TEM study, it was also observed that some of the Cu(0)-nanoparticles were found to be larger than the pore size of the support, which may be due to the presence of Cu(0)-nanoparticles on the outer



(A)



(B)



(C)

Fig. 3 (A) A SEM image of the surface of AT-Mont.; (B) EDX analysis of the surface; (C) EDX spot analysis of pores (indicated by an arrow in (A)).

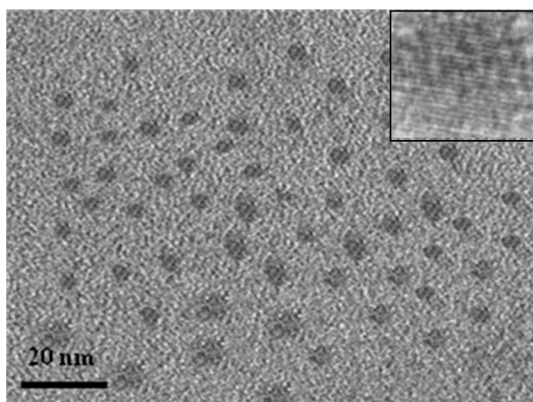


Fig. 5 TEM and HRTEM (inset) images of Cu(0)-nanoparticles.

surface of the support rather than inside the pores. The HRTEM image (Fig. 5(inset)) of a single Cu(0)-nanoparticles showed the reticular lattice planes inside the nanoparticles and these planes are continuously extended to the whole particle without any stacking faults or twins, indicating the single crystalline nature.

SEM-EDX analysis also substantiated the formation of Cu(0)-nanoparticles on the well-tuned pores of the AT-Mont. (Fig. 6(A)). Furthermore, EDX analysis (Fig. 6(B)) indicates that Cu is present on the surface of modified montmorillonite along with other elements of clay.

The appreciable decrease of the specific surface area and the specific pore volume after supporting Cu(0)-nanoparticles (Table 1) might be due to clogging of some pores by Cu(0)-nanoparticles. In addition, the presence of Cu(0)-nanoparticles may cause complexities in porosity measurement with nitrogen sorption, because the electrostatic forces between an adsorbate (*i.e.* nitrogen) and the metallic surface may affect the measured values to some extent. However, increase of pore diameter may be due to rupture of some smaller pores to generate bigger ones during the formation of Cu(0)-nanoparticles into the pores.

The Cu content in Cu(0)-Mont. as analyzed by ICP-AES, reveals the presence of 0.05 mol % of Cu in the catalyst.

3.3. Catalytic activity

The conditions for the “Click” reaction were optimized by using 1-azidodecane and phenylacetylene as model substrates. We first investigated the effect of solvent on the reaction, the mixture of water and DCM (1 : 1) is our first choice at room temperature, here we obtained about 80% yield. After that we have tried for other solvents like methanol, ethanol *etc.* and finally we used water as a solvent and surprisingly the reaction gives the highest conversion (95%) among all the solvents tested (Table 2, entries 1a–1e). Therefore, water clearly stands out as the solvent of our choice by considering its high yield, selectivity, cheapness, “green” solvent nature and environmental acceptability. Two blank experiments were also carried out between the model substrates in the presence of catalyst with or without Et₃N to understand the importance of Et₃N for the reaction to take place (Table 2, entry 1b). Therefore, the most appropriate reaction conditions in which our catalyst proceed efficiently, are in the presence of Et₃N and with water as a solvent at room temperature.

Using the optimized reaction conditions, we explored the versatility and limitations of various substrates as well as the efficiency of our catalyst for the 1,3-dipolar cycloaddition of azides and terminal alkynes to give 1,2,3-triazoles and the results are summarized in Table 3. In this study, we used various structurally and electronically diverse selected azides *e.g.* 1-azidodecane, 1-azidoadamantane, 1,6-diazidohexane and alkynes *e.g.* phenylacetylene, 1-heptyne, 1,6-heptadiyne and all the substrates produce the expected triazoles with very good to excellent yields and selectivity irrespective of nature of the substrates. The phenylacetylene (entries 1 and 3) gives higher isolated yield than linear terminal alkyne, *viz.* 1-heptyne (entries 2 and 4) with both the monoazides, *viz.* 1-azidodecane (entries 1 and 2) and 1-azidoadamantane (entries 3 and 4). Among the two monoazides, 1-azidodecane shows marginally higher conversion than 1-azidoadamantane with both the alkynes. Next, we explored our methodology for the synthesis of symmetrical bis-triazoles by coupling of dialkyne, *viz.* 1,6-heptadiyne with 1-azidodecane and 1-azidoadamantane (entries 5 and 6) and bisazide, *viz.* 1,6-diazidohexane with phenylacetylene and 1-heptyne (entries 7 and 8). As expected, in all the cases, the desired

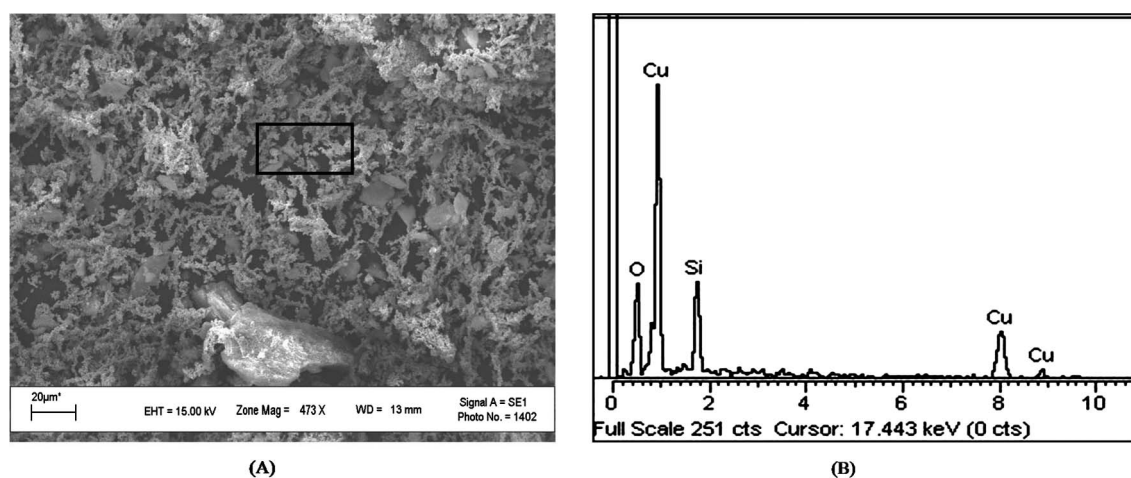


Fig. 6 (A) A SEM image of the surface of AT-Mont. after supporting the Cu(0)-nanoparticles (B) EDX spot analysis of the pores.

bis-triazoles are formed with good isolated yield (85–92%) but the reactions needed a comparatively longer time *i.e.* 1.5 h for completion.

It is worth mentioning that, under the standard reaction conditions, all reactions are highly regioselective towards 1,4-disubstituted triazoles. Simple workup operations involving filtration and crystallisation or solvent evaporation were generally applied, furnishing the corresponding 1,2,3-triazoles in excellent isolated yields.

The recyclability of our catalyst was investigated in the cycloaddition of phenylacetylene and 1-azidodecane (entry 1) and 1-azidoadamantane and 1,6-heptadiyne (entry 6). The catalyst was recovered by a simple filtration technique after each experiment. The recovered catalyst was washed with acetone, dried in a desiccator and reused directly with fresh reaction mixture without further purification for the desired 1,2,3-triazole synthesis up to the 3rd run. The results (Table 3, entries 1 and 6) showed that the catalyst remain active for several run without significant loss in efficiency. The recovered catalyst was further investigated through N_2 adsorption-desorption and powder XRD studies. The specific surface areas of the recovered catalysts decrease marginally compared to $299 \text{ m}^2 \text{ g}^{-1}$ of freshly prepared catalyst (Table 1). The BJH pore size distribution curves of the recovered catalysts retain almost same distribution pattern compared to the fresh catalyst, indicating the robustness of the catalyst (Fig. 7). The decrease of surface area of the recovered catalysts after each reaction may be due to the blockage of pores by the reactant molecules. In the powder XRD of recovered catalyst (Fig. 8), the appearance of low intensity broad peaks at around the 2θ values 36 and 54° , along with other characteristic peaks of metallic Cu, indicates the formation of a small amount of CuO after the 1st run of the reaction.^{8e} However, the efficiency of the recycled catalyst was found to be almost unaffected although a fraction of Cu(0) is converted to

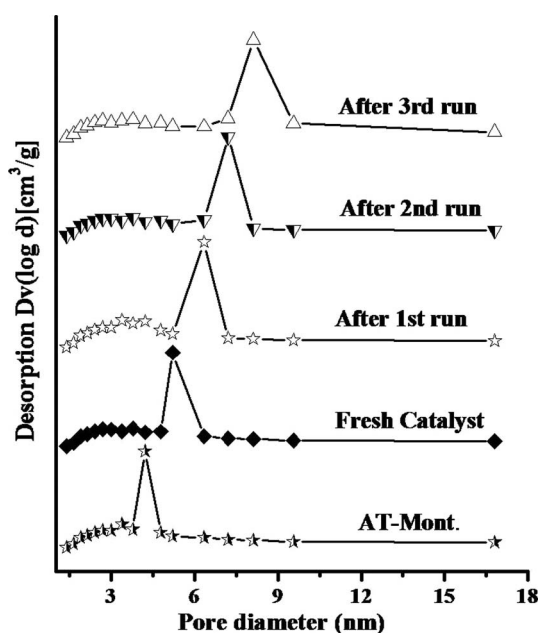


Fig. 7 BJH pore size distribution curves of AT-Mont., Fresh and Recovered catalysts.

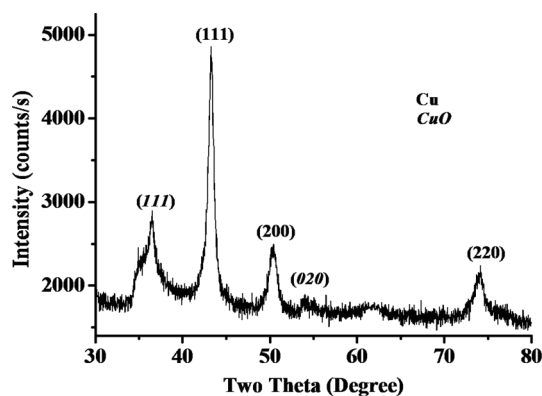


Fig. 8 The powder XRD pattern of recovered catalyst.

CuO. Such efficiency of mixed Cu/CuO nanoparticles for the “Click” reaction is also documented in the literature.^{8e}

The reaction mechanism in the azide-alkyne cycloaddition catalysed by Cu(0)-nanoparticles is not well established.⁸ The formation of Cu(I)-alkylidene complex on the surface of nanoparticles is believed to be the active species, which further combined with the azide group to give a 1,2,3-triazole.⁸ The drastic reduction in catalyst amount as well as reaction time in the reactions is possibly due to the presence of highly active Cu(0)-nanoparticles as the catalyst. The presence of robust and high surface area ($422 \text{ m}^2 \text{ g}^{-1}$) modified montmorillonite as support for Cu(0)-nanoparticles also might have a beneficial effect on the rate and regioselectivity of the reaction.

4. Conclusion

The specific surface area and the pore diameter as well as the pore size distribution of montmorillonite were tuned by controlled acid activation. The pores provided the space for nanoparticle formation and limited the growth of the particles up to the desired nano size range. Electron microscopic and spectroscopic data confirmed the formation of Cu(0)-nanoparticles into the pores of the micro- and mesoporous support. The Cu(0)-nanoparticles were spherical in shape and size in the range 0–10 nm. These nanoparticles demonstrated high catalytic activity in promoting 1,3-dipolar cycloaddition reactions between terminal alkynes and azides to synthesize highly regioselective 1,4-disubstituted mono- and bis-1,2,3-triazoles in excellent yields at room temperature in water. Further, the nanocatalysts were reused for a new batch of reactions without significant loss of their activity under the same conditions. The operational simplicity and robustness of the catalyst, as well as environmentally friendly reaction conditions, make it attractive not only for the large scale synthesis of this class of biologically active molecules, but also for the exploration in the synthesis of important drug intermediates.

Acknowledgements

The authors are grateful to Dr P. G. Rao, Director, CSIR-North East Institute of Science and Technology, Jorhat, Assam, India, for his kind permission to publish the work. The authors also thank Council Scientific and Industrial Research (CSIR), New Delhi, India, for financial support (Network project:

NWP 0010). Thanks are also due to Dr H. C. Bajaj, Scientist, CSMCRI, Bhavnagar for arranging the ICP-AES experiment. The authors BJB and PPS are grateful to CSIR, New Delhi for providing SRF.

References

- (a) H. Goessmann and C. Feldmann, *Angew. Chem., Int. Ed.*, 2010, **49**, 1362; (b) G. Schmid and B. Corain, *Eur. J. Inorg. Chem.*, 2003, 3081; (c) C. N. R. Rao, G. U. Kulkarni, P. J. Thomas and P. P. Edwards, *Chem. Soc. Rev.*, 2000, **29**, 27; (d) *Metal Nanoparticles: Synthesis, Characterization and Application*, ed. D. L. Feldheim and C. A. Floss Jr, CRC Press, New York, 2002; (e) J. M. Campelo, D. Luna, R. Luque, J. M. Marinas and A. A. Romero, *ChemSusChem*, 2009, **2**, 18; (f) A. C. Templeton, W. P. Wuelfing and R. W. Murray, *Acc. Chem. Res.*, 2000, **33**, 27.
- (a) S. Wang, Z. Wang and Z. Zha, *Dalton Trans.*, 2009, 9363; (b) O. S. Ahmed and D. K. Dutta, *Langmuir*, 2003, **19**, 5540; (c) B. J. Borah, D. Dutta and D. K. Dutta, *Appl. Clay Sci.*, 2010, **49**, 317; (d) B. J. Borah, A. Yadav and D. K. Dutta, *J. Biomed. Nanotechnol.*, 2011, **7**, 152; (e) D. Dutta, B. J. Borah, L. Saikia, M. G. Pathak, P. Sengupta and D. K. Dutta, *Appl. Clay Sci.*, 2011, **53**, 650.
- (a) L. D. Rogatis, M. Cargnello, V. Gombac, B. Lorenzut, T. Montini and P. Fornasiero, *ChemSusChem*, 2010, **3**, 24; (b) K. Kaneda, T. Mitsudome, T. Mizugaki and K. Jitsukawa, *Molecules*, 2010, **15**, 8988; (c) J. Virkutyte and R. S. Varma, *Chem. Sci.*, 2011, **2**, 837; (d) A. Fukuoka and P. L. Dhepe, *Chem. Rec.*, 2009, **9**, 224.
- (a) V. V. Rostovtsev, L. G. Green, V. V. Fokin and K. B. Sharpless, *Angew. Chem., Int. Ed.*, 2002, **41**, 2596; (b) C. D. Hein, X. M. Liu and D. Wang, *Pharm. Res.*, 2008, **25**, 2216; (c) R. Alvarez, S. Velazquez, A. San-Felix, S. Aquaro, E. De Clercq, C.-F. Perno, A. Karlsson, J. Balzarini and M. J. Camarasa, *J. Med. Chem.*, 1994, **37**, 4185; (d) G. C. Tron, T. Pirali, R. A. Billington, P. L. Canonico, G. Sorba and A. A. Genazzani, *Med. Res. Rev.*, 2008, **28**, 278; (e) E. K. Moltzen, H. Pedersen, K. P. Bogeso, E. Meier, K. Frederiksen, C. Sanchez and H. L. Lembol, *J. Med. Chem.*, 1994, **37**, 4085; (f) C. L. Droumaguet, C. Wang and Q. Wang, *Chem. Soc. Rev.*, 2010, **39**, 1233; (g) S. K. Yousof, D. Mukherjee, B. Singh, S. Maity and S. C. Taneja, *Green Chem.*, 2010, **12**, 1568; (h) D. Kumar, V. B. Reddy and R. S. Varma, *Tetrahedron Lett.*, 2009, **50**, 2065; (i) C. Shao, R. Zhu, S. Luo, Q. Zhang, X. Wang and Y. Hu, *Tetrahedron Lett.*, 2011, **52**, 3782.
- (a) V. V. Rostovtsev, L. G. Green, V. V. Fokin and K. B. Sharpless, *Angew. Chem.*, 2002, **114**, 2708; (b) C. W. Tornoe, C. Christensen and M. Meldal, *J. Org. Chem.*, 2002, **67**, 3057.
- (a) G. A. Romeiro, L. O. R. Pereira, M. C. B. V. de Souza, V. F. Ferreira and A. C. Cunha, *Tetrahedron Lett.*, 1997, **38**, 5103; (b) P. K. Kadaba, B. Stanovnik and M. Tisler, *Adv. Heterocycl. Chem.*, 1984, **37**, 217.
- (a) L. Garanti and G. Molteni, *Tetrahedron Lett.*, 2003, **44**, 1133; (b) M. Moore and P. Norris, *Tetrahedron Lett.*, 1998, **39**, 7027; (c) F. Zaragoza and S. V. Petersen, *Tetrahedron*, 1996, **52**, 10823.
- (a) A. Sarkar, T. Mukherjee and S. Kapoor, *J. Phys. Chem. C*, 2008, **112**, 3334; (b) M. L. Kantam, V. S. Jaya, B. Sreedhar, M. M. Rao and B. M. Choudary, *J. Mol. Catal. A: Chem.*, 2006, **256**, 273; (c) F. Alonso, Y. Moglie, G. Radivoy and M. Yus, *Tetrahedron Lett.*, 2009, **50**, 2358; (d) F. Alonso, Y. Moglie, G. Radivoy and M. Yus, *Eur. J. Org. Chem.*, 2010, 1875; (e) G. Molteni, C. L. Bianchi, G. Marinoni, N. Santo and A. Ponti, *New J. Chem.*, 2006, **30**, 1137; (f) H. Sharghi, R. Khalifeh and M. M. Doroodmand, *Adv. Synth. Catal.*, 2009, **351**, 207; (g) H. A. Orgueira, D. Fokas, Y. Isome, P. C.-M. Chan and C. M. Baldino, *Tetrahedron Lett.*, 2005, **46**, 2911; (h) Z. Zhang, C. Dong, C. Yang, D. Hu, J. Long, L. Wang, H. Li, Y. Chen and D. Kong, *Adv. Synth. Catal.*, 2010, **352**, 1600.
- (a) V. Polshettiwar and R. S. Varma, *Green Chem.*, 2010, **12**, 743; (b) M. N. Nadagouda, V. Polshettiwar and R. S. Varma, *J. Mater. Chem.*, 2009, **19**, 2026.
- D. K. Dutta, D. Dutta, P. P. Sarmah, S. K. Bhorodwaj and B. J. Borah, *J. Biomed. Nanotechnol.*, 2011, **7**, 76.
- J. E. Gillott, *Clay in Engineering Geology*, Elsevier, Amsterdam, 1968, 1st edn, Ch. 5.
- L. Wang, A. Lu, C. Wang, X. Zheng, D. Zhao and R. Liu, *J. Colloid Interface Sci.*, 2006, **295**, 436.
- P. J. Wallis, W. P. Gates, A. F. Patti, J. L. Scott and E. Teoh, *Green Chem.*, 2007, **9**, 980.